Proceedings of IASS-IWSS 2026 — September 14-18, 2026, Turin, Italy
"R-Evolution of Shapes: Sustainability, Re-Use, and new Design Paradigms"
Annual Symposium of the International Association for Shell and Spatial Structures
3rd Italian Workshop on Shell and Spatial Structures
A. Manuello Bertetto, S. Gabriele, F. Marmo, A. Micheletti (eds.)

Design for reuse of reclaimed concrete components: a pedagogical framework

Hanbing ZHAO, Kwong Lau HUNG, Shuaizhong WANG*

* The Chinese University of Hong Kong, [S]Equilibrium Lab
Lee Shau Kee Architecture Building, Ma Liu Shui, Shatin District, New Territories, Hong Kong
shuaizhongwang@cuhk.edu.hk

Abstract

Design for Reuse (DfR) supports circular construction by extending component service life, saving embodied carbon, and reducing waste. However, computational reuse methods are commonly presented as technical workflows, with limited pedagogical guidance on integrating material inventories, performance feedback, and physical construction. This paper examines a pedagogical framework implemented in a 13-week postgraduate architecture studio involving 26 students. The framework combined parametric design, preliminary structural analysis, component matching, multi-objective optimization, embodied-carbon assessment, joint development, and model-scale prototyping. Three projects (layout-, stress-, and geometry-driven) were compared across design, structural, and environmental criteria. Within these cases, the regular orthogonal configuration achieved the most favorable structural, reuse, carbon, and joint-repeatability performance. In contrast, the non-orthogonal two- and three-dimensional configurations supported greater spatial and geometric exploration but presented greater challenges for structural feasibility and joint development. These findings highlight the potential and limitations of reclaimed reinforced-concrete components and the need to connect geometric exploration with iterative structural assessment, component rematching, and joint development.

Keywords: design for reuse, reclaimed reinforced concrete, architectural education, structural design, multi-objective optimization

1. Introduction

Circular construction has emerged as an important approach for reducing raw material consumption, construction waste and embodied carbon in the built environment [1] – [3]. However, concrete waste from construction and demolition is still predominantly crushed and reprocessed, thereby destroying the original geometry and structural function of components, forfeiting their embodied value, and generating additional processing impacts [2]. Design for reuse (DfR) offers a higher-value alternative by extending the service life of reclaimed reinforced-concrete (RC) beams, columns, slabs, walls, and blocks while retaining their component-level geometry and potential structural capacity and reducing the demand for new materials and waste processing [3] – [6].

The reuse of reclaimed RC components nevertheless presents substantial technical and design challenges. Existing components have variable dimensions, uncertain material properties, undocumented reinforcement layouts and potentially accumulated damage. They must therefore be inventoried, inspected and assessed before being matched or adapted to new structural requirements and incorporated through reversible connection systems [4] – [7]. Unlike conventional design, in which new structural elements can be manufactured to suit a predetermined geometry, design with reclaimed

Copyright © 2026 by Hanbing ZHAO, Kwong Lau HUNG, Shuaizhong WANG
Published by the International Association for Shell and Spatial Structures (IASS) with permission.

components requires the available material stock to inform spatial, structural and assembly decisions from the outset.

Computational methods can support this stock-constrained design process. Existing studies have used parametric modelling to bring component availability and dimensional constraints into early-stage design, and matching or optimization algorithms to allocate elements by geometric and performance requirements [8] – [12]. However, these methods are commonly presented as technical workflows only, requiring designers to separately coordinate competing objectives such as architectural geometry, spatial quality, structural behavior, material efficiency, embodied carbon, and connection feasibility.

These challenges have important implications for architectural education. Related pedagogy has explored circular-design studios emphasizing systems thinking and learning through making [13], material-driven computational teaching embedding physical constraints into form generation [14], structural pedagogy connecting analysis with intuitive force–geometry relationships [15], and parametric FEM linked with physical models or design-build approaches [16], [17]. However, these areas are generally taught separately, leaving limited guidance for integrating circular material stocks, structural analysis, matching, environmental evaluation, and physical assembly within a single architectural workflow.

This paper addresses this gap by presenting an integrated digital-to-physical pedagogical framework that connects computational design, structural assessment, reuse integration, and physical prototyping for DfR of reclaimed RC components. Accordingly, the study asks: How can an integrated computational pedagogy support architecture students in applying DfR with reclaimed RC components?

The framework is examined through three contrasting student projects, representing layout-, stress-, and geometry-driven strategies, to show how computational methods can integrate reclaimed-component constraints across the design workflow, while physical prototyping extends the process towards joint development and assembly. The comparison further identifies a gap between generating computational performance outputs and using them to inform iterative design improvement.

2. Methods

This study used a case-study approach to examine the application of a DfR pedagogical framework in an architecture studio.

2.1. Studio framework

The framework was implemented in a 13-week postgraduate architecture studio involving 26 students in autumn 2025, treating reclaimed RC components as early design inputs that informed form, structure, component allocation, and assembly. The studio was organized in two stages (Fig. 1): design generation and performance evaluation in Stage 1, through parametric form-finding, preliminary structural assessment, component matching, multi-objective optimization, and embodied-carbon calculation; and reuse integration and physical translation in Stage 2, through joint design, constructability studies, and physical prototyping.

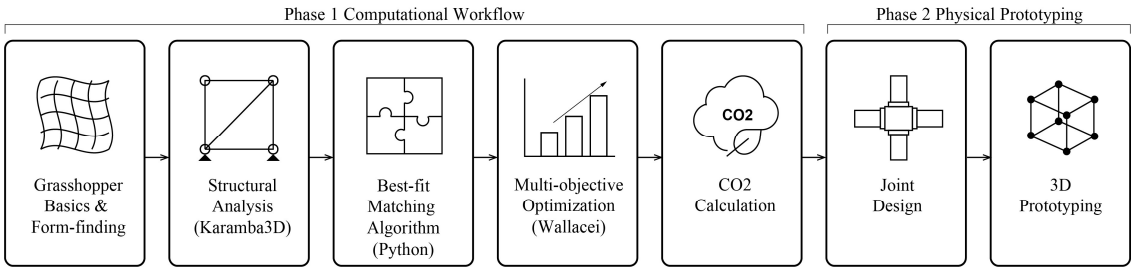


Figure 1: The pedagogical workflow for DfR of reclaimed RC components.

2.2. Digital-to-physical workflow

A predefined material bank was extracted from digital models of Tong Lau buildings at 230–232 and 352–354 Ma Tau Wai Road. It comprised 271 RC columns and 650 RC beams, documented by cross-sectional dimensions, reusable lengths, and quantities. Column widths, depths, and reusable lengths ranged from 250–610 mm, 300–1,120 mm, and 2,110–4,930 mm, respectively; the corresponding beam ranges were 230–690 mm, 380–1,220 mm, and 60–5,770 mm. All components were assigned an RC20 material model in Karamba3D (E = 30 GPa; specific weight = 25 kN/m³; tensile strength = 10 MPa; compressive strength = 13 MPa). Reinforcement layouts and component-specific conditions were not modelled, so the inventory served as a pedagogical dataset.

Students were encouraged to develop parametric proposals in Grasshopper using Magnetizing Floorplan Generator, Lunchbox, Kangaroo, and Karamba3D. After conceptual form generation, preliminary Karamba3D analysis examined load paths and established the minimum cross-sectional requirements for target beams and columns used in component matching.

A customized Python-based Best-Fit algorithm assigned inventory components to target members by comparing cross-sectional dimensions and lengths, while calculating matching and cut-off ratios. Wallacei then supported multi-objective optimization using project-specific objectives, including matching efficiency, material use, spatial quality, solar performance, and carbon impact.

Following component assignment, the structural models were updated using the cross-sections of the matched components and analyzed again in Karamba3D. The stress-to-strength ratio was the principal post-matching indicator, with −1 to 1 adopted as the evaluation range. Schemes exceeding this range were classified as structurally unresolved, requiring resizing, rematching, or structural-system revision.

The estimated net embodied-carbon saving was calculated as:

$$EE = \left(V_{c,\mathrm{reused}} - V_{c,\mathrm{new}}\right)F_c - V_{s,\mathrm{new}}F_s \tag{1}$$

where EE is the estimated net embodied-carbon saving (kg CO_2e); $V_{c,\mathrm{reused}}$, $V_{c,\mathrm{new}}$, and $V_{s,\mathrm{new}}$ are the volumes of reused concrete, newly added concrete, and newly added steel (m³), respectively; and F_c and F_s are the emission factors for concrete and steel. These were set at 369 and 15,072 kg CO_2e/m^3, respectively. Reused concrete was credited against equivalent new-concrete production; demolition, transport, and end-of-life stages were excluded. Positive values indicate estimated savings, whereas negative values indicate that the impacts of newly added materials exceeded the credited reuse benefit.

To account for differences in the projected scale of the selected schemes, EE was divided by the horizontal projected area:

$$I_{\mathrm{EE}} = \frac{EE}{A_P} \tag{2}$$

where I_{EE} is the area-normalised net embodied-carbon saving (kg CO_2e/m^2) and A_P is the horizontal projected area of the selected scheme (m²). This accounts for size differences but not functional or structural equivalence among proposals.

The concrete reuse ratio was calculated as:

$$R_{\mathrm{reuse}} = \frac{V_{c,\mathrm{reused}}}{V_{c,\mathrm{reused}} + V_{c,\mathrm{new}}} \times 100\% \tag{3}$$

where $V_{c,\mathrm{reused}}$ and $V_{c,\mathrm{new}}$ are the volumes of reused and newly added concrete. R_{reuse} denotes the share of design concrete supplied by the material bank, not the share of the donor inventory reused.

Following the intermediate review, the students collectively selected six of the twelve initial schemes for further development through joint design and physical prototyping. The prototypes combined 3D-printed geometry and connection components with concrete casting to represent reclaimed RC elements

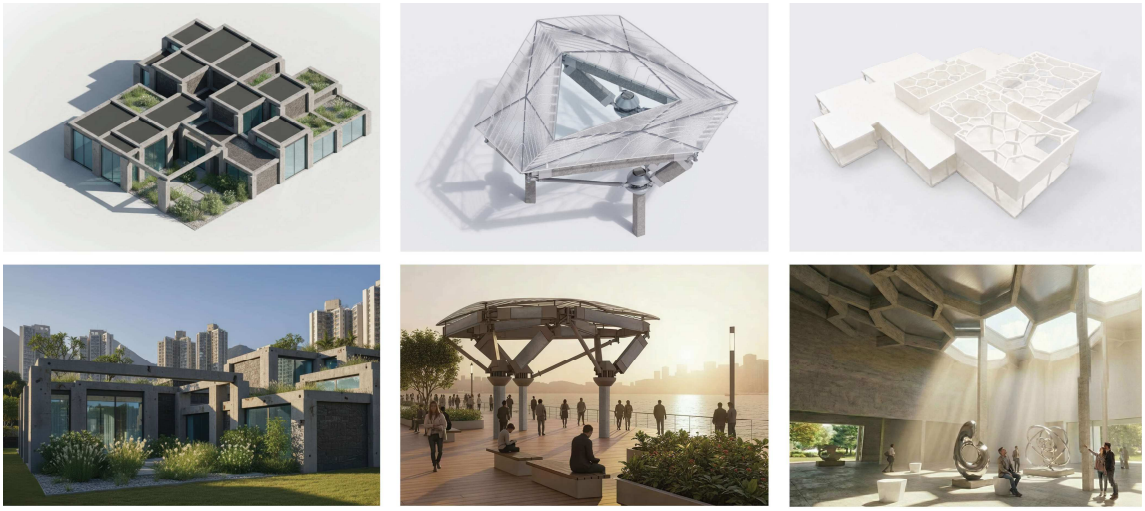
at model scale, examining geometric translation, joint articulation, tolerance, and assembly sequence rather than structural capacity.

2.3. Case evaluation

Three of the six developed schemes were purposively selected as contrasting layout-, stress-, and geometry-driven cases. Evaluation drew on design booklets, computational outputs, connection drawings, and physical models. As summarized in Figure 9, the cases were assessed separately across design, structure, and environment, without aggregation into a composite score. Design integration, representation, and joint repeatability were qualitatively rated as high, moderate, or low from the submitted evidence. Structural status was determined using the post-matching criterion defined in Section 2.2, while reuse and carbon performance were reported using R_{reuse} and I_{EE}. The symbols provide a visual summary of the recorded or assessed outcomes rather than externally validated performance thresholds; consequently, strengths in one domain do not offset unresolved structural performance in another.

3. Results

The three cases completed the principal stages of the digital-to-physical workflow, but produced different architectural, material, environmental, structural, and tectonic outcomes. The comparison therefore separates workflow achievement from preliminary engineering performance.



a. Layout-driven Design b. Stress-driven Design c. Geometry-driven Design

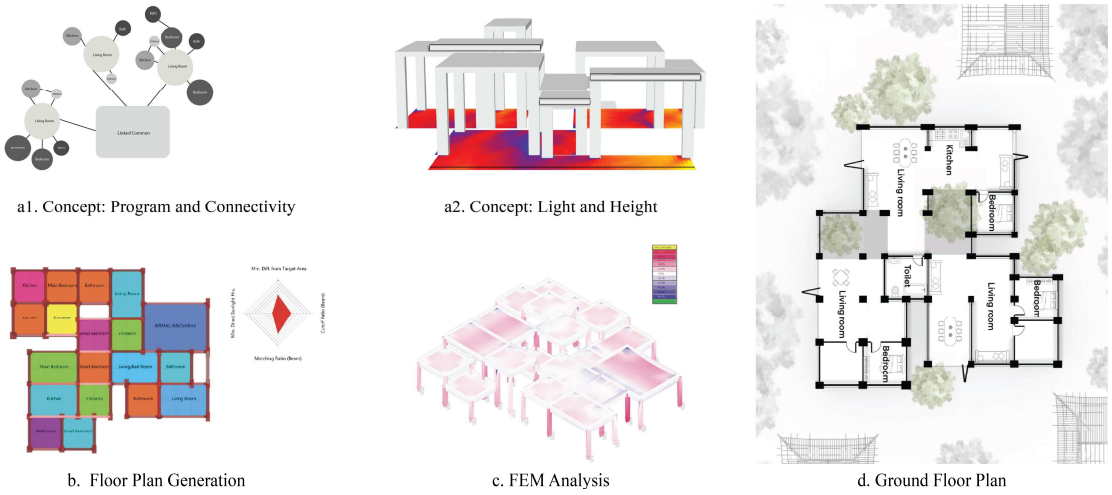
Figure 2: Three representative design outcomes. (a) Layout-driven residential prototype; (b) stress-line-driven pavilion; and (c) geometry-driven Voronoi roof. The upper row shows overall geometry, while the lower row shows spatial renderings. Image credits: (a) Tsz Ching FUNG, Shing Hin HO, Ka Yi CHAN, Orso Maria BONETTI; (b) Hou Lam YU, Hau Yee CHOW, Kam Lok CHAN, Chun Kwan TAI; (c) Chun Nok CHOW, Ka Hei LAI, Kin Hei TSANG, Long Ki WONG, Siu Yeung WU.

3.1. Design strategies

The three selected cases comprise a layout-driven residential prototype, a stress-driven pavilion, and a geometry-driven Voronoi roof (Fig. 2). The layout-driven residential prototype was developed as a low-rise community frame (Fig. 2a; Fig. 3). Drawing on the spatial logic of local walled villages, its parametric model coordinated programme adjacency, circulation, frame layout, component allocation, and direct sunlight. The stress-driven pavilion used stress lines derived from a loaded slab to generate a demountable canopy (Fig. 2b; Fig. 4). Principal force trajectories informed its subdivision and inclined members, while solar shading and the central opening were included in the multi-objective search. The

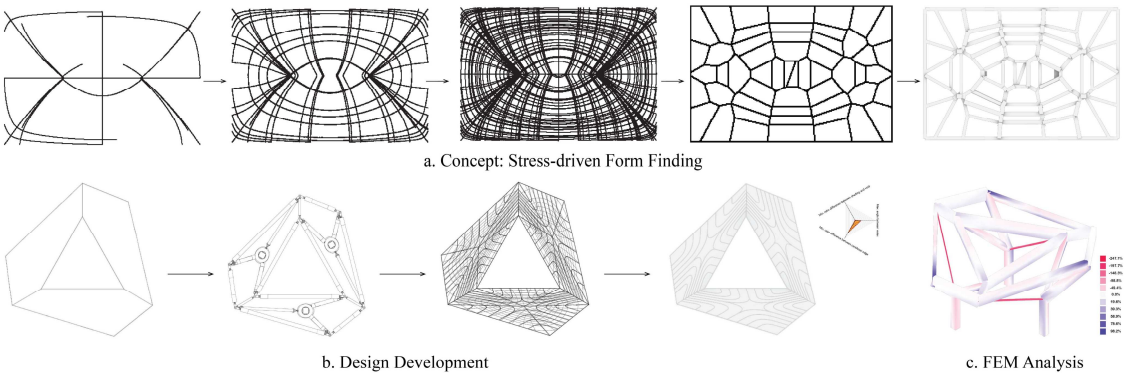
geometry-driven case used Voronoi subdivision and geometric relaxation to form a museum roof around an atrium and galleries (Fig. 2c; Fig. 5). Cell spacing, roof openings, daylight shafts, spatial relationships, and reclaimed-component matching were explored together.

The cases demonstrate three computational emphases within the same DfR workflow. The layout-driven case began with spatial organization and stock allocation, the stress-driven case with force trajectories, and the geometry-driven case with a spatial roof pattern. They are compared to examine how these different starting points affected the coordination of architectural, material, environmental, structural, and tectonic criteria, rather than establish an overall ranking.



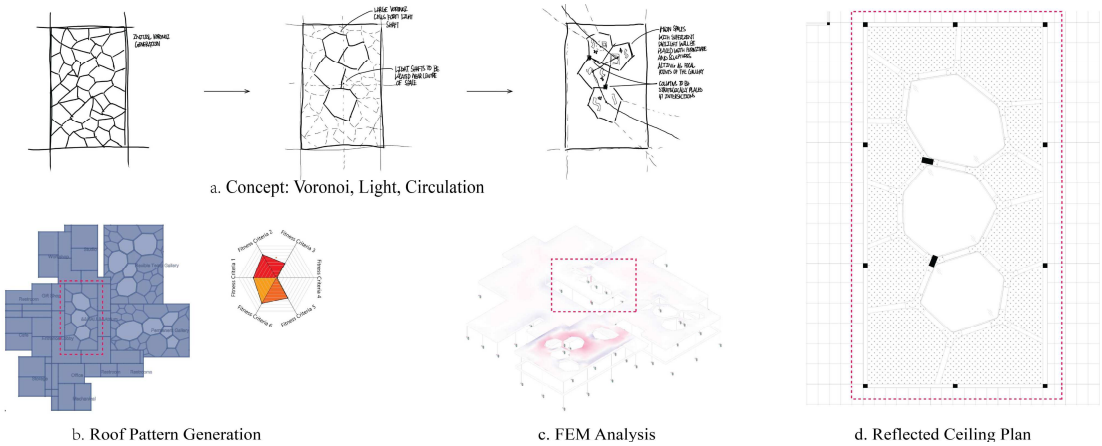
a1. Concept: Program and Connectivity
a2. Concept: Light and Height
b. Floor Plan Generation
c. FEM Analysis
d. Ground Floor Plan

Figure 3: Magnetizing-based layout generation links programme adjacency, circulation, sunlight access, and reclaimed component matching. Image credits: Tsz Ching FUNG, Shing Hin HO, Ka Yi CHAN, Orso Maria BONETTI.



a. Concept: Stress-driven Form Finding
b. Design Development
c. FEM Analysis

Figure 4: Translation of Karamba3D stress analysis into principal force trajectories. Image credits: Hou Lam YU, Hau Yee CHOW, Kam Lok CHAN, Chun Kwan TAI.



a. Concept: Voronoi, Light, Circulation

b. Roof Pattern Generation

c. FEM Analysis

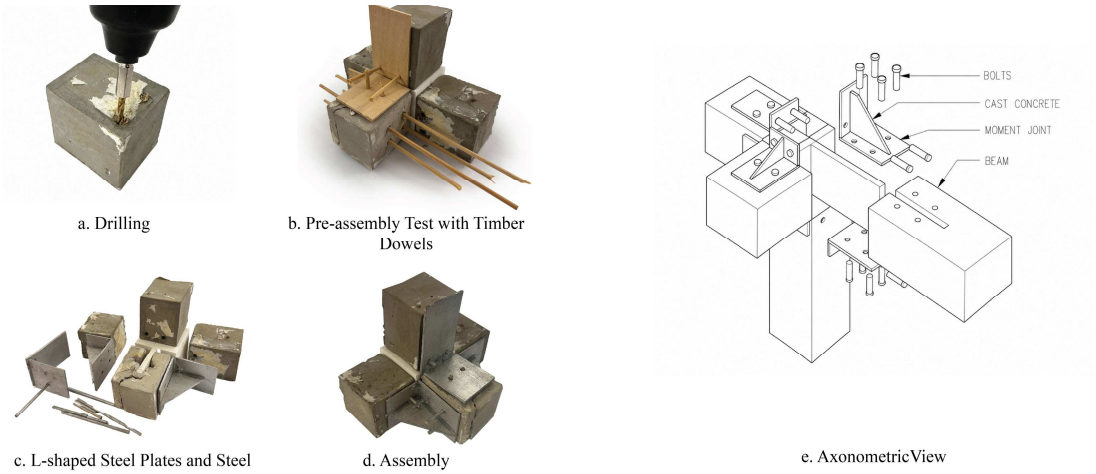
d. Reflected Ceiling Plan

Figure 5: Voronoi subdivision and geometric relaxation generated roof openings, daylight shafts, and ceiling variation for a museum roof system. Image credits: Chun Nok CHOW, Ka Hei LAI, Kin Hei TSANG, Long Ki WONG, Siu Yeung WU.

3.2. Tectonic translation

Joint design connected the computational reuse strategies with model-scale physical assembly. Across the three cases, steel plates, bolts, sleeves, hubs, and cast interfaces were introduced to address component alignment, angular variation, assembly tolerance, and connection detailing. The prototypes examined joint geometry and assembly logic rather than structural capacity.

The layout-driven case used L-shaped steel plates, bolts, and local cast-concrete interfaces to form an orthogonal cruciform joint (Fig. 6). Its regular geometry enabled a repeatable assembly sequence, although drilling and casting could interfere with existing reinforcement and limit reversibility. The stress-driven case used beam-to-beam connectors and a stiffened circular steel hub to connect inclined members to the column (Fig. 7). Rotational interfaces accommodated variations in member angles but increased fabrication and tolerance demand. The geometry-driven case used steel sleeves and anchor bolts around a reinforced central skeleton to connect members at irregular Voronoi intersections (Fig. 8). This accommodated multidirectional geometry but required node-specific detailing and local adjustment. Within the three cases, increasing geometric irregularity was accompanied by lower joint standardization and greater assembly complexity.



a. Drilling

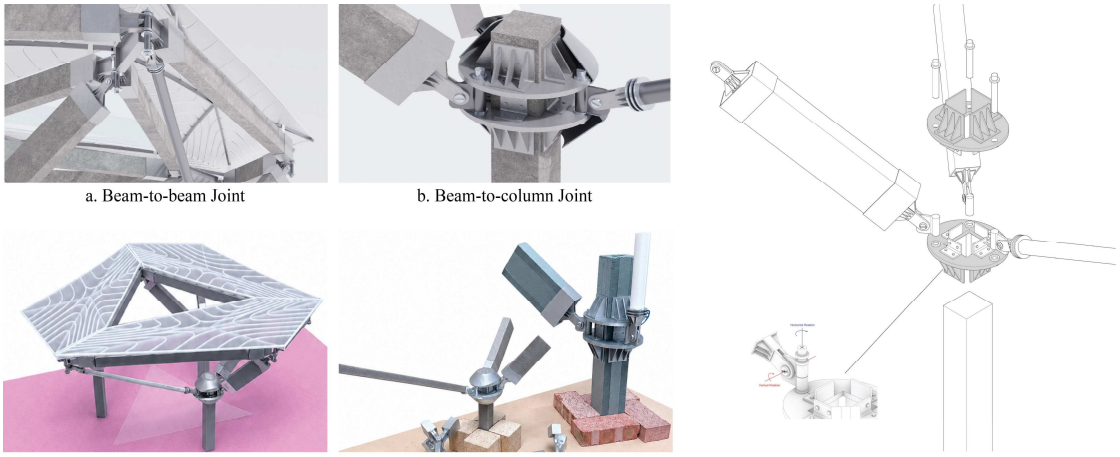
b. Pre-assembly Test with Timber Dowels

c. L-shaped Steel Plates and Steel

d. Assembly

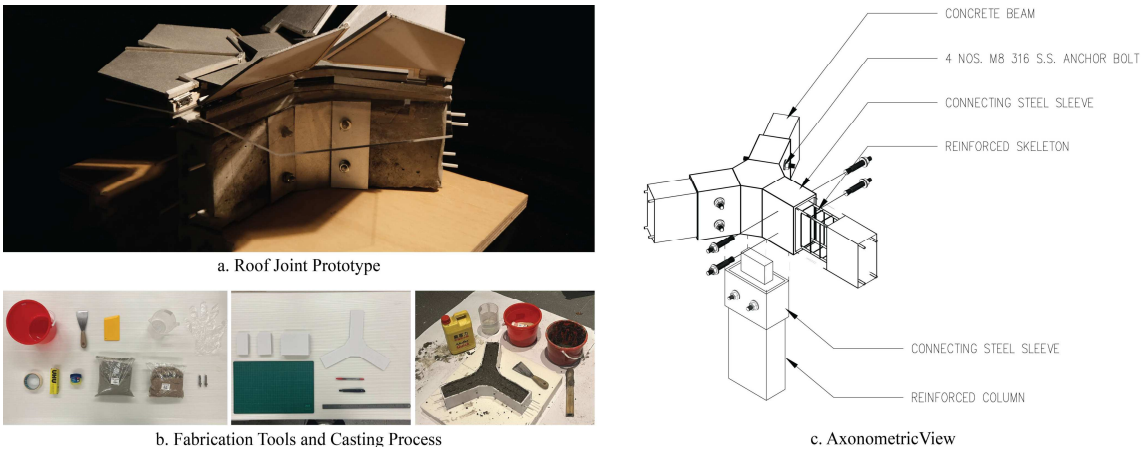
e. AxonometricView

Figure 6: Orthogonal cruciform joint using L-shaped steel plates, dowels, and bolts. Image credits: Tsz Ching FUNG, Shing Hin HO, Ka Yi CHAN, Orso Maria BONETTI.



a. Beam-to-beam Joint b. Beam-to-column Joint c. Overall Pavilion Pototype d. Beam-to-column Joint Evolution e. AxonometricView

Figure 7: Multidirectional steel hub with sleeves and rotational interfaces connecting inclined members. Image credits: Hou Lam YU, Hau Yee CHOW, Kam Lok CHAN, Chun Kwan TAI.



a. Roof Joint Prototype b. Fabrication Tools and Casting Process c. AxonometricView

Figure 8: Sleeve-and-bolt joint and casting process for the non-orthogonal Voronoi roof. Image credits: Chun Nok CHOW, Ka Hei LAI, Kin Hei TSANG, Long Ki WONG, Siu Yeung WU.

3.3. Cross-case performance

Figure 9 compares the three cases across design, structural, and environmental criteria. The qualitative ratings indicate relative differences among the selected cases, while the quantitative indicators retain their calculated values. Because the projects differed in function, scale, geometry, and design objectives, the results were interpreted as multidimensional performance profiles rather than aggregated into a composite score.

The projected areas of the layout-, stress-, and geometry-driven schemes were 235, 77, and 180 m², respectively. Their estimated net embodied-carbon savings (EE) were +44,299, +160, and −49,757 kg CO_2e, corresponding to area-normalised values (I_{EE}) of +188.5, +2.1, and −276.4 kg CO_2e/m².

The layout-driven case combined spatial layout with sunlight analysis through a 2.5D configuration. It demonstrated moderate structural concept integration and relatively limited design representation but achieved the strongest measured performance. Its stress-to-strength ratio of −0.62 to 0.81 remained within the adopted range of −1 to 1, and its regular joint configuration provided high repeatability. It also achieved the highest concrete reuse ratio, at 84.2%, and I_{EE} is +188.5 kg CO_2e/m².

The stress-driven case translated force-flow analysis into a three-dimensional geometry and demonstrated high structural concept integration and design representation. Its adjustable hub joint provided moderate repeatability, and its concrete reuse ratio reached 67.3%. However, its stress-to-strength ratio ranged from −50.31 to 50.17, substantially exceeding the adopted range. Its I_{EE} was marginally positive at +2.1 kg CO_2e/m^2. This result shows that integrating structural concepts into form generation did not necessarily produce a structurally resolved final scheme.

The geometry-driven case used a two-dimensional Voronoi configuration to coordinate geometry with sunlight response. It demonstrated high design representation but limited structural concept integration and low joint repeatability because its connections required node-specific adjustment. It achieved the lowest concrete reuse ratio, at 42.7%, and a negative I_{EE} of −276.4 kg CO_2e/m^2. Its stress-to-strength ratio of −2.47 to 0.98 also exceeded the adopted range, indicating that the scheme remained structurally unresolved.

As a result, the comparison distinguishes design and representational achievement from measured performance. The stress- and geometry-driven cases demonstrated stronger design representation, whereas the layout-driven case achieved more favorable structural, joint-repeatability, reuse, and I_{EE} outcomes. The findings therefore show that incorporating structural concepts into architectural form did not by itself ensure satisfactory post-matching structural performance.

	Design A (layout-driven)	**Design B (stress-driven)**	**Design C (geometry-driven)**
DESIGN			
Design strategy	Layout + Sunlight	Force flow	Voronoi + Sunlight
Geometric configuration	2.5D	3D	2D
Structural concept integration	◐ moderate	● high	○ low
Design representation	○ low	● high	● high
STRUCTURE			
Stress-to-strength ratio (-1.00 to 1.00)	-0.62 to 0.81	-50.31 to 50.17 (unsolved)	-2.47 to 0.98 (unsolved)
Joint repeatability	● high	◐ moderate	○ low
ENVIRONMENT			
R_{reuse} (%)	84.2	67.3	42.7
I_{EE} (kg CO_2e/m^2)	+188.5	+2.1	-276.4

Figure 9: Cross-case evidence matrix showing the performance profiles of the three selected designs.

4. Discussion and conclusion

The findings indicate that incorporating reclaimed components and performance analysis into the design workflow is insufficient for DfR education unless the results inform iterative design revision. Students need to interpret the feedback and revise their proposals accordingly. Structural concepts embedded in form generation did not necessarily lead to structurally resolved outcomes after component matching. Future studios should therefore introduce explicit decision gates requiring students to resize or rematch components, or revise the structural system, before proceeding to joint development and physical prototyping.

The comparison additionally suggests that reclaimed-component availability, structural requirements, architectural geometry, and connection logic should be coordinated early. Geometric irregularity may increase matching, fabrication, tolerance, and assembly demands. Joint repeatability and assembly sequence should therefore become criteria during form generation and optimization rather than remain downstream detailing tasks.

The study contributes an integrated pedagogical framework that connects circular construction, computational design, performance assessment, component matching, and physical translation. It demonstrates the value of treating reclaimed RC components as early design constraints while distinguishing design achievement from measured performance. However, the study remains exploratory. The material inventory lacked reinforcement, condition, and traceability data. The model-scale prototypes did not verify structural capacity or constructability at full scale. The carbon assessment excluded several life-cycle stages. In addition, the layout-based optimization remained largely planar. Producing complex, non-standard joints for components of different dimensions and orientations presented further difficulties. The limited studio duration restricted students' ability to master multiple computational tools.

Future research should incorporate component testing, material passports, uncertainty classification, full-scale joint validation, and more consistent performance documentation. Three-dimensional structural geometries should be explored beyond plan-oriented configurations. Parametric joint studies could generate and evaluate connections between components of different dimensions and orientations. Further research could examine whether specific geometries are better suited to particular reclaimed materials. For example, Voronoi systems could be more compatible with lightweight, machinable linear materials such as timber than with reclaimed RC components [18]. In conclusion, DfR can be taught as a design logic that connects architectural intention with material availability, structural feedback, environmental assessment, and assembly feasibility.

Acknowledgements

The authors thank the 26 postgraduate students of the Autumn 2025 course Topical Studies in Building Technology: Reuse as Design for their contributions.

References

[1] I. Amarasinghe, Y. Hong, and R. A. Stewart, "Development of a material circularity evaluation framework for building construction projects," *Journal of Cleaner Production*, vol. 436, p. 140562, Jan. 2024, doi: 10.1016/j.jclepro.2024.140562.

[2] A. T. M. Marsh, A. P. M. Velenturf, and S. A. Bernal, "Circular economy strategies for concrete: implementation and integration," *Journal of Cleaner Production*, vol. 362, p. 132486, Aug. 2022, doi: 10.1016/j.jclepro.2022.132486.

[3] I. Bertin, M. Saadé, R. Le Roy, J.-M. Jaeger, and A. Féraille, "Environmental impacts of design for reuse practices in the building sector," *Journal of Cleaner Production*, vol. 349, p. 131228, May 2022, doi: 10.1016/j.jclepro.2022.131228.

[4] J. Devènes, J. Brütting, C. Küpfer, M. Bastien-Masse, and C. Fivet, "Re:Crete – Reuse of concrete blocks from cast-in-place building to arch footbridge," *Structures*, vol. 43, pp. 1854–1867, Sep. 2022, doi: 10.1016/j.istruc.2022.07.012.

[5] J. Devènes, M. Bastien-Masse, and C. Fivet, "Reusability assessment of reinforced concrete components prior to deconstruction from obsolete buildings," *Journal of Building Engineering*, vol. 84, p. 108584, May 2024, doi: 10.1016/j.jobe.2024.108584.

[6] C. Küpfer, M. Bastien-Masse, and C. Fivet, "Reuse of concrete components in new construction projects: Critical review of 77 circular precedents," *Journal of Cleaner Production*, vol. 383, p. 135235, Jan. 2023, doi: 10.1016/j.jclepro.2022.135235.

[7] C. Küpfer, N. Bertola, and C. Fivet, "Reuse of cut concrete slabs in new buildings for circular ultra-low-carbon floor designs," *Journal of Cleaner Production*, vol. 448, p. 141566, Apr. 2024, doi: 10.1016/j.jclepro.2024.141566.

[8] M. B. Eschenbach et al., "Matter as met: Towards a computational workflow for architectural design with reused concrete components," in *Towards Radical Regeneration*, C. Gengnagel, O. Baverel, G. Betti, M. Popescu, M. R. Thomsen, and J. Wurm, Eds. Cham, Switzerland: Springer International Publishing, 2023, pp. 442–455, doi: 10.1007/978-3-031-13249-0_35.

[9] Y. Huang, L. Alkhayat, C. De Wolf, and C. Mueller, "Algorithmic circular design with reused structural elements: Method and tool," in *Proceedings of the International fib Symposium on the Conceptual Design of Structures*, vol. 55, 2021, pp. 457–468, doi: 10.35789/fib.PROC.0055.2021.CDSymp.P056.

[10] A. Bukauskas, P. Shepherd, P. Walker, B. Sharma, and J. Bregulla, "Form-fitting strategies for diversity-tolerant design," in *Proceedings of the IASS 2017 Symposium: Interfaces: Architecture, Engineering, Science*, Hamburg, Germany, Sep. 25–28, 2017, pp. 1–10. [Online]. Available: https://people.bath.ac.uk/ps281/research/publications/hamburg_preprint5.pdf

[11] J. Brütting, G. Senatore, M. Schevenels, and C. Fivet, "Optimum design of frame structures from a stock of reclaimed elements," *Frontiers in Built Environment*, vol. 6, Art. no. 57, May 2020, doi: 10.3389/fbuil.2020.00057.

[12] D. Marshall, C. Mueller, B. Clifford, and S. Kennedy, "Computational arrangement of demolition debris," *Detritus*, no. 11, pp. 3–18, Jul. 2020, doi: 10.31025/2611-4135/2020.13967.

[13] E. Campbell, C. Niblock, N. Flood, and S. Lappin, "Introducing circularity in early architectural design education," *Archnet-IJAR: International Journal of Architectural Research*, vol. 19, no. 4, pp. 888–903, Sep. 2024, doi: 10.1108/ARCH-03-2024-0094.

[14] S. Abdelmohsen and P. Massoud, "A material-based computation framework for parametric design education," *Open House International*, vol. 46, no. 3, pp. 459–475, Jul. 2021, doi: 10.1108/OHI-02-2021-0043.

[15] S. Wang, "Structural design pedagogy under the embodied perception: An equilibrium-based approach for architecture students," in *Proceedings of the IASS 2024 Symposium: Redefining the Art of Structural Design*, Zurich, Switzerland, Aug. 26–30, 2024. [Online]. Available: https://app.iass2024.org/files/IASS_2024_Paper_167.pdf

[16] M. Dall'Igna and M. S. Oliveira, "Correlated physical and parametric FEM modeling for computational design and engineering workflows: A way to facilitate understanding of structural behavior," in *Proceedings of the IASS 2024 Symposium: Redefining the Art of Structural Design*, Zurich, Switzerland, Aug. 26–30, 2024. [Online]. Available: https://app.iass2024.org/files/IASS_2024_Paper_361.pdf

[17] G. M. Avinç, "Design-build projects in architecture education and experimental structures as a pedagogical approach," *Journal of Engineering Science and Technology Review*, vol. 17, no. 4, pp. 228–239, Aug. 2024, doi: 10.25103/jestr.174.25.

[18] H. Hua, L. Hovestadt, and P. Tang, "Optimization and prefabrication of timber Voronoi shells," *Structural and Multidisciplinary Optimization*, vol. 61, no. 5, pp. 1897–1911, May 2020, doi: 10.1007/s00158-019-02445-x.